

# Plasmoid behavior in LHD plasmas

Ryuichi ISHIZAKI and Noriyoshi NAKAJIMA

National Institute for Fusion Science, Toki 509-5292, Japan

In order to clarify the difference on the motion of a plasmoid created by a pellet injection between tokamak and helical plasmas, MHD simulation including ablation processes has been carried out. In LHD plasma, the plasmoid drifts to the lower field side similarly to tokamak. However, it is found that the drift direction is reversed after several Alfvén transit times in the case that the plasmoid is located at the inner side of the torus on the horizontal elongated poloidal cross section.

Keywords: pellet, drift, tire tube force, MHD, CIP

## 1 Introduction

Injecting small pellets of frozen hydrogen into torus plasmas is a proven method of fueling [1]. The physical processes are divided into the following micro and macro stages. The micro stage is the ablation of mass at the pellet surface due to the high temperature bulk plasma which the pellet encounters. The neutral gas produced by the ablation is rapidly heated by electrons and ionized to form a high density and low temperature plasma, namely a plasmoid. The macro stage is the redistribution of the plasmoid by free streaming along the magnetic field lines and by MHD processes which cause mass flow across flux surfaces. The micro stage is well-understood by an analytic method [2] and numerical simulation [3]. The drift motion of the plasmoid is investigated in the macro stage [4]. Since the plasmoid drifts to the lower field side, the pellet fueling to make the plasmoid approach the core plasma has succeeded by injecting the pellet from the high field side in tokamak. On the other hand, such a good performance has not been obtained yet in the planar axis heliotron; Large Helical Device (LHD) experiments, even if a pellet has been injected from the high field side [5]. The purpose of the study is to clarify the difference on the motion of the plasmoid between tokamak and helical plasmas.

In order to investigate the motion of the plasmoid, the three dimensional MHD code including the ablation processes has been developed by extending the pellet ablation code (CAP) [3]. It was found through the comparison between simulation results and an analytical consideration that the drift motion to the lower field side in tokamak is induced by a tire tube force due to the extremely large pressure of the plasmoid and a  $1/R$  force due to the magnetic pressure gradient and curvature in the major radius direction as shown in Ref. [6]. In the study, the motion of the plasmoid is investigated in the LHD plasma in four cases that the plasmoids are initially located at the inner and outer sides of the torus on the vertical and horizontal elongated poloidal cross sections. The plasmoids drift

to the lower field sides in all cases. However, in the case that it is located at the inner side of the torus on the horizontal elongated poloidal cross section, it is found that the drift direction is reversed after several Alfvén transit times, namely it drifts to the higher field side.

## 2 Basic Equations

Since the plasmoid is such a large perturbation that the linear theory can not be applied, a nonlinear simulation is required to clarify the behavior of the plasmoid. The drift motion is considered to be a MHD behavior because the drift speed obtained from experimental data [1] is about several % of  $v_A$ , where  $v_A$  is an Alfvén velocity. Thus, the three dimensional MHD code including the ablation processes has been developed by extending the pellet ablation code (CAP) [3]. The equations used in code are:

$$\frac{d\rho}{dt} = -\rho \nabla \cdot \mathbf{u}, \quad (1a)$$

$$\rho \frac{d\mathbf{u}}{dt} = -\nabla p + \mathbf{J} \times \mathbf{B} + \nu \rho \left[ \frac{4}{3} \nabla (\nabla \cdot \mathbf{u}) - \nabla \times \omega \right], \quad (1b)$$

$$\frac{dp}{dt} = -\gamma p \nabla \cdot \mathbf{u} + (\gamma - 1) \left[ H + \eta J^2 + \nu \rho \left( \frac{4}{3} (\nabla \cdot \mathbf{u})^2 + \omega^2 \right) \right], \quad (1c)$$

$$\frac{\partial \mathbf{B}}{\partial t} = \nabla \times (\mathbf{u} \times \mathbf{B} - \eta \mathbf{J}), \quad (1d)$$

$$\mathbf{J} = \nabla \times \mathbf{B}, \quad (1e)$$

$$\omega = \nabla \times \mathbf{u}. \quad (1f)$$

$\rho$ ,  $\mathbf{B}$ ,  $\mathbf{u}$  and  $p$  are normalized by  $\rho_0$ ,  $B_0$ ,  $v_A$  and  $B_0^2/\mu_0$  at the magnetic axis, respectively, where  $\mu_0$  is the magnetic permeability.  $\gamma = 5/3$ ,  $\nu = 10^{-6} v_A L_0$  and  $\eta = 10^{-6} \mu_0 v_A L_0$  are used as the ratio of the specific heats, viscosity and

author's e-mail: ishizaki@nifs.ac.jp

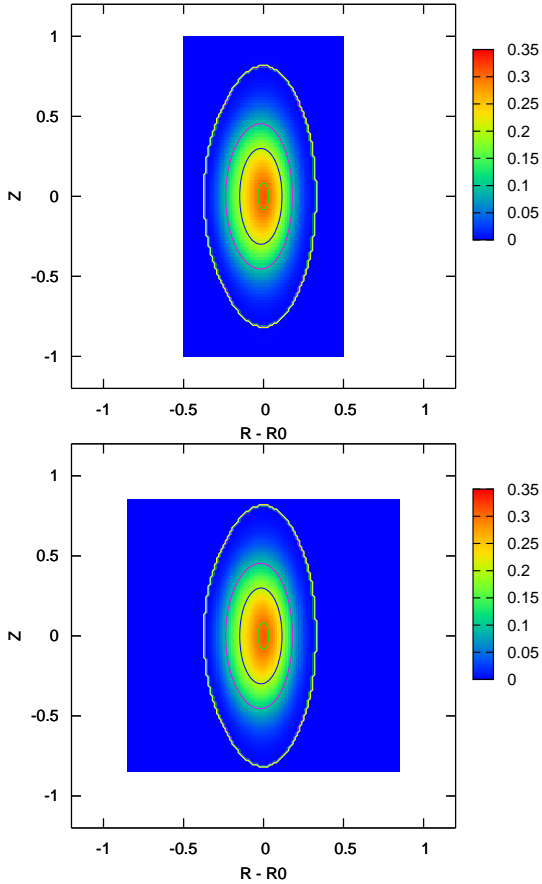


Fig. 1 Pressure contours on the vertical elongated poloidal cross sections at  $\phi = 0$  in (a) the HINT and (b) the CAP codes expressing the LHD plasma with  $R_0 = 3.82$ . The last closed surfaces are defined by the contour lines of 0.5% of the maximum pressure.

electric resistivity, respectively, where  $L_0$  is a characteristic length; 1 m. Heat source  $H$  is given by:

$$H = \frac{dq_+}{dl} + \frac{dq_-}{dl}, \quad (2)$$

where  $q_{\pm}$  is the heat flux model dependent on electron density and temperature in the bulk plasma and the plasmoid density.  $l$  is the distance along the field line. The subscript + (-) refers to the electrons going to the right (left). Then, the heat source can be calculated on each field line. Assuming Maxwellian electrons incident to the plasmoid, a kinetic treatment using a collisional stopping power formula leads to the heat flux model,  $q_{\pm}$  [3] which is used in construction of the ablation model [2].

In order to investigate the plasmoid motion in LHD plasmas, an equilibrium obtained by the HINT code [7] is used as the bulk plasma. Although the HINT code uses the rotational helical coordinate system, the CAP code uses the cylindrical coordinate system  $(R, \phi, Z)$  because of preventing numerical instability induced by a locally and extremely large perturbation of the plasmoid. The colors in Figs. 1(a) and (b) show the pressure contours in the

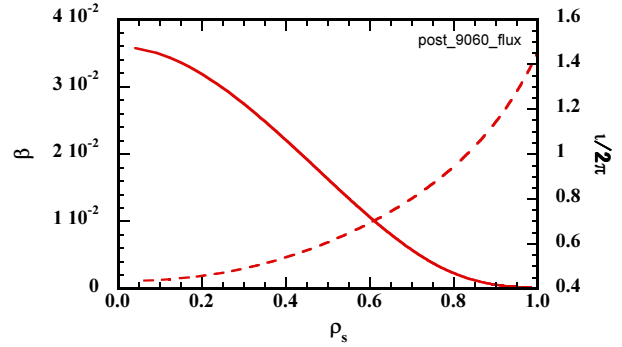


Fig. 2 The plasma beta  $\beta$  (solid line) and rotational transform  $l/2\pi$  (dashed line) as a function of normalized minor radius  $\rho_s$  in the LHD plasma.

poloidal cross sections at  $\phi = 0$  in the HINT and CAP codes, respectively. The yellow lines show the last closed surfaces defined by the contour line of 0.5% of the maximum pressure. The domain of the CAP code is larger than one of the HINT code because it is necessary for the last closed surface to be within the simulation box. In other words, the HINT code can not provide all data required by the CAP. Equations (1) are thus solved only in the inside of the last closed surface in the CAP code. Therefore, it is difficult to evaluate accurately the plasmoid motion around the last closed surface, but it is possible to carry out more stable simulation than one in the rotational helical coordinate. The Cubic Interpolated Pseudoparticle (CIP) method is used in the code as a numerical scheme [8].

### 3 Drift motion of plasmoid in LHD plasma

When a plasmoid is heated in tokamak plasmas, it is expanding along the magnetic field and simultaneously drifts to the lower field side due to a tire tube force and a  $1/R$  force induced by the magnetic field with curvature [6]. In the study, the motion of the plasmoid is investigated in the LHD plasma. Figure 2 shows the plasma beta  $\beta$  and rotational transform  $l/2\pi$  in the bulk plasma as a function of normalized minor radius  $\rho_s$  used in the code. Figure 3 show four initial locations of the plasmoids. The colors in Figs. 3(a) and (b) show the pressure contours in the poloidal cross sections at  $\phi = 0$  (vertical elongated one) and  $2\pi/20$  (horizontal elongated one), respectively. The plasmoids denoted by circles A and C are located at the inner side of the torus, and those denoted by circles B and D are located at the outer side of it. Namely, the plasmoid A is at the highest field side and the plasmoid D is at the lowest field side among them. Those plasmoids are located on the same flux surface of  $\rho_s = 0.4$ , which is corresponding to  $l/2\pi = 0.54$  as shown in Fig. 2. The peak values of density and temperature of the plasmoid are 1000 times

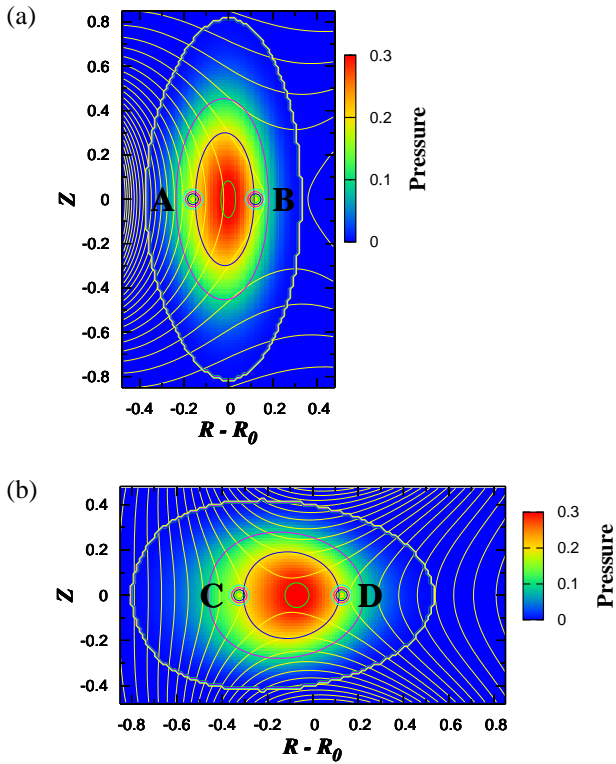


Fig. 3 Four initial locations of the plasmoids in the LHD plasma with  $R_0 = 3.82$ . The colors show the pressure contours in the poloidal cross sections at (a)  $\phi = 0$  (vertical elongated one) and (b)  $\phi = 2\pi/20$  (horizontal elongated one). The last closed surfaces are defined by the contour lines of 0.5% of the maximum pressure. The yellow lines show the contour of the magnetic pressure. The plasmoids denoted by circles A, B, C and D are located on the same flux surface of  $\rho_s = 0.4$ .

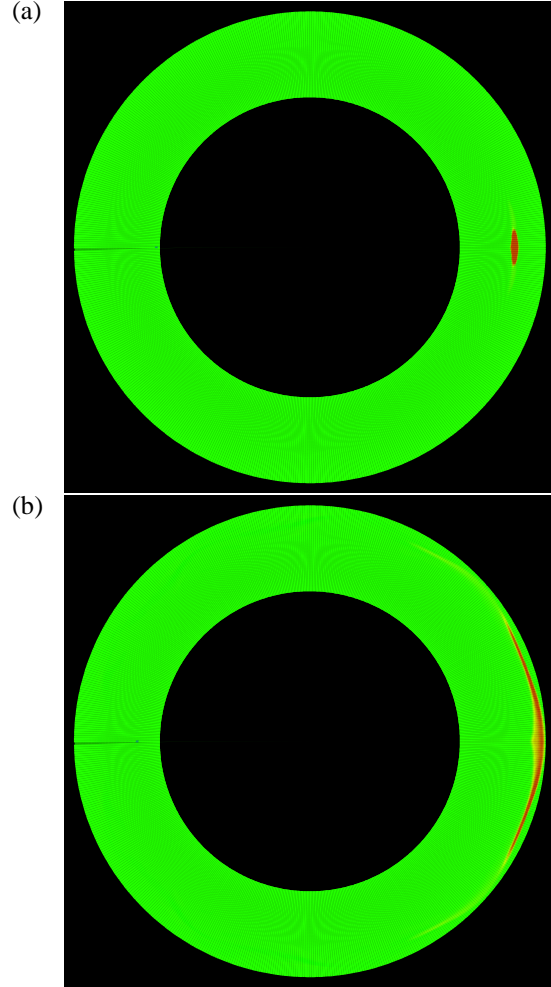


Fig. 5 The projection of the density in the direction of Z of the plasmoid D at (a)  $t = 2\tau_A$  and (b)  $t = 10\tau_A$ .

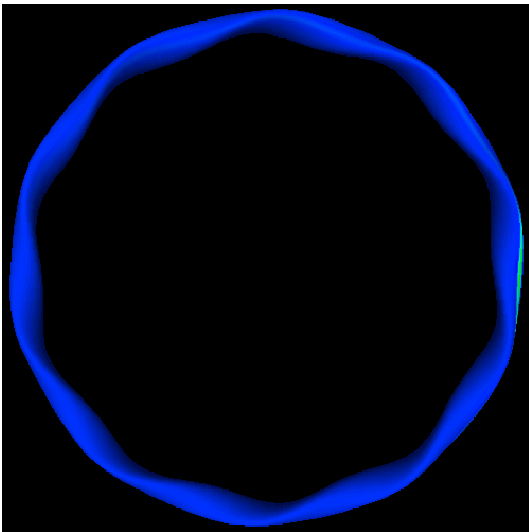


Fig. 4 The contour of the mass flow  $\rho u_r$  of the plasmoid D across the flux surface  $\rho_s = 0.4$  at  $t = 5\tau_A$ .

density and 1/1000 times temperature of the bulk plasma, respectively. The plasmoid, whose half width is 0.03, encounters the electrons with fixed temperature 2 keV and density  $10^{20} \text{ m}^{-3}$ .

Simulations have been carried out in four cases A, B, C and D. Figure 4 shows the contour of the mass flow  $\rho u_r$  of the plasmoid D across the flux surface  $\rho_s = 0.4$  at  $t = 5\tau_A$ , where  $\tau_A$  is the Alfvén transit time. Figures 5(a) and (b) show the projection of the density in the direction of Z at  $t = 2\tau_A$  and  $10\tau_A$ , respectively, of the plasmoid D. It is found from Figs. 4 and 5 that the plasmoid is expanding along the magnetic field line with about 10% of the Alfvén velocity and simultaneously drifts across the flux surface in the direction of the major radius with about 1% of the Alfvén velocity. Figures 6(a) and (b) are the averaged density and averaged mass flow on the flux surfaces, respectively, of the plasmoid A (red line) and B (blue line). Solid and dashed lines show ones at  $t = 2\tau_A$  and  $10\tau_A$ , respectively. The plasmoid A drifts toward the magnetic axis because it drifts to the lower field side due to the tire tube and  $1/R$  forces. Thus, the mass flow becomes negative, and

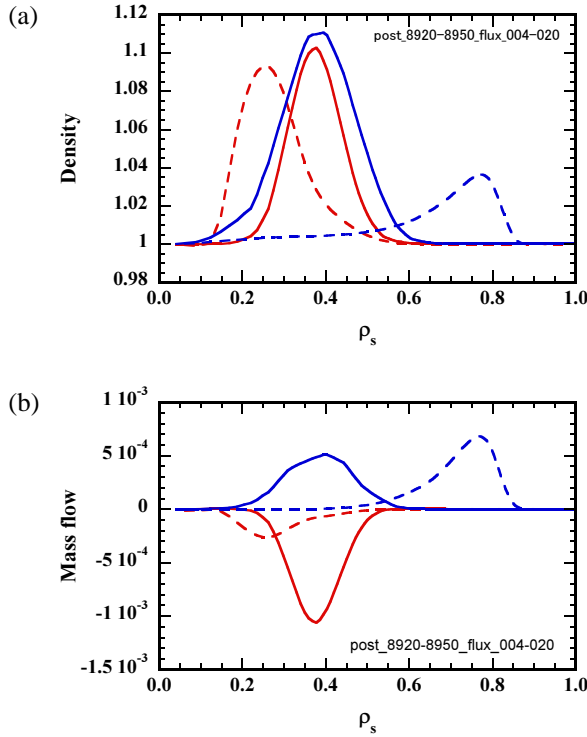


Fig. 6 (a) The averaged density and (b) the averaged mass flow on the flux surfaces as a function of the normalized minor radius,  $\rho_s$ . Red and blue lines show ones of the plasmoid A and B, respectively. Solid and dashed lines show ones at  $t = 2\tau_A$  and  $10\tau_A$ , respectively.

the peak density drifts in the negative direction of  $\rho_s$ . Since the plasmoid B is initially located in the region where the gradient of the magnetic pressure is negative because a saddle point of one is at  $R - R_0 \sim 0.27$  as shown in Fig. 3(a), it drifts in the direction of the major radius. Thus, the mass flow becomes positive, and the peak density drifts in the direction of  $\rho_s$ . Figures 7(a) and (b) are the averaged density and averaged mass flow on the flux surfaces, respectively, of the plasmoid C (red line) and D (blue line). Solid and dashed lines show ones at  $t = 2\tau_A$  and  $10\tau_A$ , respectively. The plasmoid C had a positive mass flow at  $t = 2\tau_A$ , but it has a negative one at  $10\tau_A$ . Namely, the plasmoid drifts in the negative direction of the major radius, and subsequently drifts in the positive direction of it. Since the plasmoid C is initially located in the region where the gradient of the magnetic pressure is positive, it is reasonable that the plasmoid drifts in the negative direction of the major radius at first. The plasma beta of the plasmoid becomes  $\sim 1$  because the magnetic well is induced by the extremely large pressure. Therefore, the drift direction is considered to be reversed due to the change of the magnetic pressure and curvature induced by such a high beta. The detail will be clarified in the future work. The plasmoid D located in the lowest field side among the four cases drifts in the direction of the major radius. The mass flow thus becomes positive and the peak of the density drifts in the direction

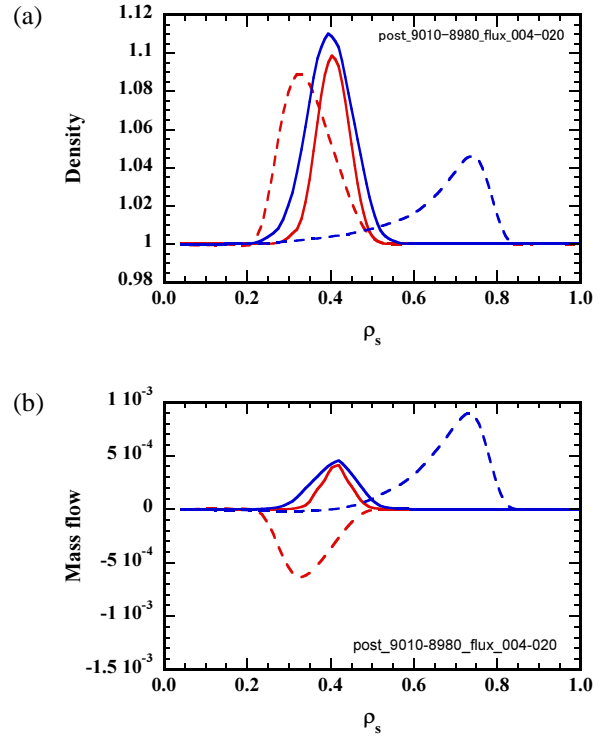


Fig. 7 (a) The averaged density and (b) the averaged mass flow on the flux surfaces as a function of the normalized minor radius,  $\rho_s$ . Red and blue lines show ones of the plasmoid C and D, respectively. Solid and dashed lines show ones at  $t = 2\tau_A$  and  $10\tau_A$ , respectively.

of  $\rho_s$ .

## 4 Summary

It is verified by simulations using the CAP code that the plasmoid with a high pressure induced by heat flux drifts to the lower field side for several Alfvén transit times in the LHD plasma. Such a drift is induced by a tire tube force and  $1/R$  force caused by an extremely large pressure of the plasmoid similarly to tokamak. However, it is found that the drift direction is reversed in the case that an initial location of the plasmoid is the inner side of the torus on the horizontal elongated poloidal cross section. That fact is considered to be caused by the change of the magnetic pressure and curvature induced by the high beta, but the detail analysis will be required to clarify the physics mechanism.

- [1] Y. W. Muller et al. Nucl. Fusion, **42**, 301 (2002).
- [2] P. B. Parks and M. N. Rosenbluth. Phys. Plasmas, **5**, 1380 (1998).
- [3] R. Ishizaki et al. Phys. Plasmas, **11**, 4064 (2004).
- [4] P. B. Parks et al. Phys. Rev. Lett., **94**, 125002 (2005).
- [5] R. Sakamoto et al. in proceedings of 29th EPS conference on Plasma Phys. and Control. Fusion.
- [6] R. Ishizaki et al. IAEA-CN-149/TH/P3-6 (2006).
- [7] K. Harafuji et al. J. Comp. Phys., **81**, 169 (1989).
- [8] H. Takewaki et al. J. Comput. Phys., **61**, 261 (1985).